

# Disambiguation of Human Intent Through Control Space Selection

Deepak E. Gopinath\* · Brenna D. Argall

Received: date / Accepted: date

**Abstract** Assistive shared-control robots have the potential to transform the lives of millions of people afflicted with severe motor impairments as a result of spinal cord or brain injuries. The effectiveness and usefulness of shared-control robots is closely related to their ability to infer the user’s needs and intentions and is often a limiting factor for providing appropriate assistance quickly, confidently and accurately. The contributions of this paper are three-fold: first, we propose a goal disambiguation algorithm which enhances the intent inference and assistive capabilities of a shared-control assistive robotic arm. Second, we introduce a novel intent inference algorithm that works in conjunction with the disambiguation scheme, inspired by *dynamic field theory* in which the time evolution of the probability distribution over goals is specified as a dynamical system. Third, we present a pilot human subject study to evaluate the efficacy of the disambiguation system. This study was performed with eight subjects. *Results show that upon operating the robot in the control mode picked by the disambiguation algorithm, the progress towards the goal became significantly faster as a result of accurate and*

*confident robot assistance, and the number and rate of mode switches performed by the user decreased as well.*

**Keywords** Shared Autonomy · Intent Inference · Intent Disambiguation · Assistive Robotics

**Acknowledgements** This material is based upon work supported by the National Science Foundation under Grant CNS 15544741. Any opinions, findings and conclusions or recommendations expressed in this material are those of the authors and do not necessarily reflect the views of the aforementioned institutions.

## 1 Introduction

Assistive and rehabilitation machines—such as robotic arms and smart wheelchairs—have the potential to transform the lives of millions of people with severe motor impairments (LaPlante et al, 1992). These machines can promote independence, boost self-esteem and help to extend the mobility and manipulation capabilities of such individuals, and revolutionize the way motor-impaired people interact with society (Scherer, 1996; Huete et al, 2012). With the rapid technological strides in the domain of assistive robotics, the machines have become more capable and complex, and with this complexity the control of these machines has become a greater challenge.

The control of an assistive machine is typically enacted through a control interface. Moreover, the greater the motor impairment of the user, the more limited are the interfaces available for them to use. These interfaces (for example, sip-and-puffs and switch-based head arrays) are low-dimensional, discrete interfaces that can operate only in subsets of the entire control space (Simpson et al, 2008; Nuttin et al, 2002). The dimensionality mismatch between the control interfaces

---

Deepak E. Gopinath  
Department of Mechanical Engineering  
Northwestern University, Evanston, IL  
Shirley Ryan AbilityLab, Chicago, IL.  
E-mail: deepakgopinath@u.northwestern.edu

Brenna D. Argall  
Department of Mechanical Engineering, Electrical Engineering  
and Computer Science,  
Northwestern University, Evanston, IL,  
Department of Physical Medicine and Rehabilitation, Northwestern University, Chicago, IL,  
Shirley Ryan AbilityLab, Chicago, IL.  
E-mail: brenna.argall@northwestern.edu

\* Corresponding Author

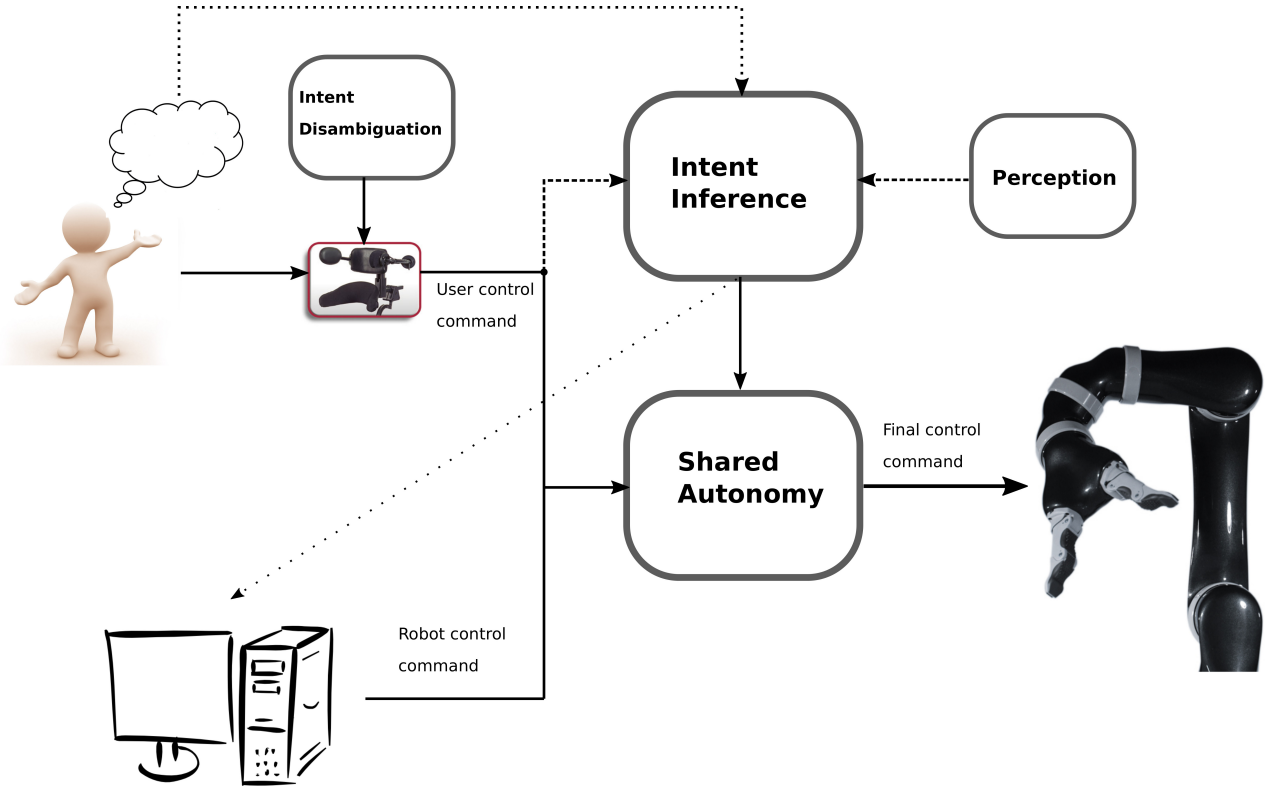


Fig. 1 Core components of a shared control architecture.

and the controllable degrees-of-freedom of the assistive robot necessitates the partitioning of the entire control space into smaller subsets called *control modes*. Moreover, the more limited and lower-dimensional the control interface, the greater the number of control modes. In order to achieve full control of the machine, the user must switch between the control modes, which is referred to as *mode switching* or *modal control*. Mode switching adds to the cognitive and physical burden of task execution and has a detrimental effect on the performance (Eftring and Boschian, 1999). The introduction of *shared autonomy* to these assistive machines seeks to alleviate some of these issues. In a shared control system the task responsibility is shared between the user and the robot, with the aim of reducing human effort in achieving a goal. Shared autonomy systems arbitrate between the human control commands and the autonomous control commands using different strategies depending on the task context, user preference and robotic platform. Figure 1 depicts the key components of a typical shared control architecture.

Any assistive robotic system needs to have a good idea of the user’s needs and intentions. Therefore, intent inference is a necessary and crucial component to ensure appropriate assistance. In assistive robotic manipulation specifically, often the first step of a manipulation task is to reach for and grasp discrete objects in the

environment. Intent inference therefore can be frames as a problem of estimating a probability distribution of intent likelihood over all possible goals (objects) in the environment. This inference is usually informed by various cues from the human and the environment, such as the human control actions, biometric measures that indicate the cognitive and physical load of the user during task execution and task-relevant features such as robot and goal locations. With a greater number of sensor modalities available, it is likely that the intent inference becomes more accurate.

However, in the assistive domain, user acceptance and adoption is of paramount importance. Adding more sensors to track biometric data and object locations can become expensive or impractical (e.g. if the sensor must be worn by the user). For reasons of user adoption and cost, we intentionally design our assistance add-ons to be as invisible and close to the manual system as possible. The information we are able to capture from the human therefore is largely restricted to the control commands they issue to the assistive machine. Sparsity and noise in these control commands make the inference task even harder, prompting the need for robust intent inference formalisms.

Our key insight is that certain control commands issued by the human are *more intent expressive* than others, and may help the autonomy in inference accuracy.

This is the notion of *inverse legibility* (Gopinath and Argall, 2017) in which human-generated actions *help the robot* to infer the human’s intent unambiguously. Consider the hypothetical reaching experiment illustrated in Figure 2. Since the spatial locations of the goals are maximally spread along the horizontal axis, any human control command issued along the horizontal dimension conveys a lot of information about the intended goal to the robot. In other words, motion along  $x$  is more *intent expressive* and will help the robot to draw accurate inference more quickly and confidently. This approach to more seamless human-robot interaction exploits the underlying implicit exchanges of information between partners that are inherent to task execution with shared intentions.

In this work, as our primary contribution we develop a mode switch assistance paradigm that enhances the robot’s intent inference capabilities, by selecting the control mode in which a user-initiated motion will *maximally disambiguate* human intent. The disambiguation layer elicits more *intent expressive* commands from the user by placing the user control in certain control modes. Furthermore, the disambiguation power of the algorithm is closely linked to, and is dependent on, the success and accuracy of the underlying intent inference mechanism. Therefore, as our secondary contribution, we also develop a novel intent inference scheme which utilizes ideas from *dynamic field theory* that efficiently incorporates information contained in past states to improve the performance of the disambiguation system.

In Section 2 we present an overview of relevant research in the areas of shared autonomy in assistive robotics, types of shared autonomy assistance paradigms, intent inference and synergies in human-robot interaction. Section 3 presents the mathematical formalism developed for intent inference and disambiguation. Section 4 focuses on the implementation details of the shared control system. The study design and experimental methods are discussed in Section 5 followed by results in Section 6. Discussion and conclusions are presented in Sections 7 and 8 respectively.

## 2 Related Work

This section provides an overview of related research in the domains of shared autonomy in assistive robotics, robot assistance for modal control, intent inference in human-robot interaction and information acquisition in robotics.

Shared-autonomy in assistive systems aims to reduce the user’s cognitive and physical burden during task execution without having the user relinquish complete control (Philips et al, 2007; Demeester et al, 2008; Gopinath

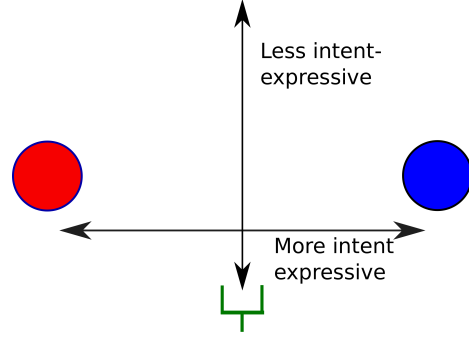


**Fig. 2** Illustration of goal disambiguation along various control dimensions. Any motion of the end effector (green) along the  $y$ -axis will not help the system to disambiguate the two goals (A and B). However, motion along the  $x$ -axis provides cues as to which goal.

et al, 2017; Muelling et al, 2017). Shared autonomy is preferred over fully autonomous robotic systems due to enhanced user satisfaction and robustness. The most common strategies to share control between the user and the assistive system include (a) hierarchical paradigms in which the higher level goals are entrusted with the user and the autonomy generates low-level control (Tsui et al, 2011; Kim et al, 2010, 2012), (b) control allocation in distinct partitions of the control space (Driessen et al, 2005) and c) blending user controls and robot autonomy commands (Downey et al, 2016; Storms and Tilbury, 2014; Muelling et al, 2017).

In order to offset the drop in task performance due to shifting focus (task switching) from the task at hand to switching between different control modes different mode switch assistance paradigms have been proposed. For example, a simple time-optimal mode switching scheme has shown to improve task performance (Herlant et al, 2016; Pilarski et al, 2012).

Shared control systems often require a good estimate of the human’s intent—for example, their intended reaching target in a manipulation task or a target location in the environment in a navigation task ((Liu et al, 2016)). Intent can either be explicitly communicated by the user (Choi et al, 2008) or can be inferred from their control signals or sensor data using various algorithms. Intent recognition and inference are actively studied by cognitive scientists and roboticists and can be broadly categorized into two main classes: model-based approaches and heuristic approaches. In model-based approaches, intent inference is typically cast within a Bayesian framework, and the posterior distribution over goals (belief) at any time is determined by the iterative application of Bayes theorem. Evidence in this context can be derived from a combination of factors such as task-relevant features in the environment, human control

actions or biometric data from the user. The user often is modeled as a Partially Observable Markov Decision Process (POMDP) (Taha et al, 2011) and is assumed to behave according to a predefined control policy that maps the states to actions. Although iterative belief updating using Bayes theorem provides an optimal strategy to combine new evidence (likelihood) with *a priori* information (prior), incorporating an extended history of past states and control actions increases the computational complexity and tractability becomes an issue. In such cases, first-order Markovian independence assumptions make the inference tractable. In heuristic approaches, the formulations are often simpler and seek to find direct mappings from instantaneous cues and the underlying human intention. For example, the use of instantaneous confidence functions for estimating intended reaching target in robotic manipulation (Dragan and Srinivasa, 2012; Gopinath et al, 2017). However, heuristic methods in general are not sophisticated enough to incorporate histories of past states and actions, making them less robust to external noise.

Eliciting more legible and information-rich control commands from the user to improve intent estimation can be thought of as an information acquisition process. Intent information acquisition can be an *active* process in which the robot takes actions that will probe the human’s intent (Sadigh et al, 2016b,a). Designing optimal control laws that maximize information gain can be accomplished by having the associated reward structure reflect some measure of information gain (Atanasov et al, 2014). Autonomous robots designed for exploration and data acquisition tasks can benefit from exploring more information-rich regions in the environment. If the spatial distribution of information density is known *a priori*, information maximization can be accomplished by maximizing the ergodicity of the robot’s trajectory with respect to the underlying information density map (Miller et al, 2016; Miller and Murphey, 2013).

By having the human assist the robot in its intent inference capacity, our work leverages the underlying synergies that are inherent in human-robot cooperation. In the context of human-human cooperative teams, the notion of shared intentionality—one in which all parties involved in a collaborative task team share the same intention or goal and have a joint commitment towards it—is crucial to make task execution more seamless and efficient (Tomasello and Carpenter, 2007; Tomasello and Moll, 2010). This principle is relevant to successful human-robot interaction as well. From the robot’s perspective, the core idea behind our disambiguation system is that of “*Help Me, Help You*”—that is, if the user can help the robot with more information-rich actions, then the robot in turn can provide accurate

and appropriate task assistance more quickly and confidently. A framework for “*people helping robots helping people*” in which the robot relies on semantic information and judgments provided by the human to improve its own capabilities has been developed in (Sorokin et al, 2010). In order to overcome the various types of communication bottlenecks that can hamper performance, different types of communication interfaces have been developed that account for the restricted capabilities of the robot (Goodfellow et al, 2010). Lastly, more intent-expressive human actions is related to the idea of legibility in robot actions. In human-robot interaction, the legibility and predictability of robot motion to the human has been investigated (Dragan et al, 2013) and various techniques to generate legible robot motion have been proposed (Holladay et al, 2014). Our work introduces the idea of *inverse legibility* (Gopinath and Argall, 2017) in which the assistance scheme is intended to bring out more legible intent-expressive control commands *from* the human.

### 3 Mathematical Formalism

This section describes our intent disambiguation algorithm that computes the control mode that can maximally disambiguate between the goals and the intent inference mechanism that works in conjunction with the disambiguation algorithm. Section 3.1 outlines the mathematical notation used in this paper. Section 3.2 describes the disambiguation algorithm. The mathematical details of the intent inference paradigms is outline in detail in Section 3.3.

#### 3.1 Notation

Let  $\mathcal{G}$  denote the set of all candidate goals with  $n_g = |\mathcal{G}|$  and let  $g^i$  refer to the  $i^{th}$  goal with  $i \in [1, 2, \dots, n_g]$ . A *goal* represents the human’s underlying intent. Specifically, in assistive robotic manipulation, since the robotic device is primarily used for reaching toward and grasping of discrete objects in the environment, intent inference is the estimation of the probability distribution over all possible goals (objects) in the environment. At any time  $t$ , the robot actively maintains a probability distribution over goals denoted by  $\mathbf{p}(t)$  such that  $\mathbf{p}(t) = [p^1(t), p^2(t), \dots, p^{n_g}(t)]^T$  where  $p^i(t)$  denotes the probability associated with goal  $g^i$ . The probability  $p^i(t)$  represent the robot’s *confidence* that goal  $g^i$  is the human’s intended goal.

Let  $\mathcal{K}$  be the set of all controllable dimensions of the robot and  $k^i$  represent the  $i^{th}$  control dimension where  $i \in [1, 2, \dots, n_k]$ . The cardinality of  $\mathcal{K}$  is denoted as

$n_k$  and typically depends on the robotic platform used. For example, for a smart wheelchair  $n_k = 2$ , since the controllable degrees-of-freedom are velocity and heading and for a six degrees-of-freedom robotic arm with a gripper  $n_k = 7$ .

The limitations of the control interfaces necessitate the control space  $\mathcal{K}$  to be partitioned into control modes. Let  $\mathcal{M}$  denote the set of all control modes with  $n_m = |\mathcal{M}|$ . Additionally, let  $m^i$  refer to the  $i^{\text{th}}$  control mode where  $i \in [1, 2, \dots, n_m]$ . Each control mode  $m^i$  is a subset of  $\mathcal{K}$  such that  $\bigcup_{i=1}^{n_m} m^i$  spans all of the controllable dimensions. Let  $\mathbf{e}^i$  be the standard basis vectors that denote the unit velocity vector along the  $i^{\text{th}}$  control dimension<sup>1</sup>. The disambiguation formalism developed in Section 3.2 is agnostic to the particular form of intent inference. However, the algorithm assumes that  $\mathbf{p}(t)$  can be forward projected in time by iteratively applying the intent inference algorithm.

The disambiguation metric that characterizes the disambiguation capabilities of a control dimension  $k \in \mathcal{K}$  is denoted by  $D_k \in \mathbb{R}$ . We explicitly define disambiguation metrics for both positive negative motions along  $k$  as  $D_k^+$  and  $D_k^-$  respectively. We also define a disambiguation metric  $D_m \in \mathbb{R}$  for each control mode  $m \in \mathcal{M}$ .  $D_m$  is a measure of how informative and useful the user control commands would be for the robot if the user were to operate the robot in control mode  $m$ . The higher it is, the easier it will be for the system to infer human's intent. Both  $D_k$  and  $D_m$  will be formally defined in Section 3.2.2.

The robot pose and the goal pose for  $g \in \mathcal{G}$  are denoted  $\mathbf{x}_r$  and  $\mathbf{x}_g$  respectively and  $\mathbf{u}_h$  denotes the human control command.

### 3.2 Intent Disambiguation

The need for intent disambiguation arises from how the probability distribution over goals evolves as the user controls the robot and moves it in space. That is, given an intent inference mechanism that is dependent on robot pose or movement (**cite TODO, refer notes**), as the user controls the robot in different control modes, the probability distribution evolves. Figure 3 shows simulations which motivate the development of a disambiguation metric. For different control modes, the confidences associated with each goal are different. Moreover, motions in some control modes result in sharper rise in some goal confidences compared to others. This

indicates the existence of control modes that can better disambiguate between the goals.

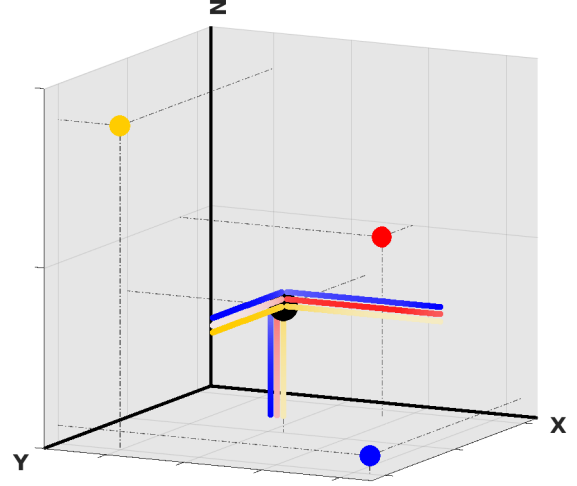


**Fig. 3** Illustration of how goal confidences change upon motion along control dimensions. The three colored lines along each dimension represent the confidences associated with a goal of corresponding color. One can see that motion along certain control dimensions result in sharper rise in confidences for some goals compared to others.

The computation of  $D_k$  depends on four components (denoted as  $\Gamma_k$ ,  $\Omega_k$ ,  $\Lambda_k$  and  $\Upsilon_k$ ), which in turn depend on a projection of the probability distribution over intent. These computations and projection are described in detail in Section 3.2.1 and Section 3.2.2, and as a pseudocode in Algorithm 1.

#### 3.2.1 Forward Projection of $\mathbf{p}(t)$

The first step towards the computation of  $D_k$  is the forward projection of the probability distribution  $\mathbf{p}(t)$  from the current time  $t_a$  to  $t_b$  and  $t_c$  ( $t_a < t_b < t_c$ ), Algorithm 1, lines 3-13). Application of control command  $\mathbf{e}^k$  results in probability distributions  $\mathbf{p}_k^+(t_b)$ ,  $\mathbf{p}_k^+(t_c)$  and  $-\mathbf{e}^k$  results in  $\mathbf{p}_k^-(t_b)$  and  $\mathbf{p}_k^-(t_c)$ . Note that Algorithm 1 is run twice, to compute the projected probability distributions for  $\mathbf{e}^k$  and  $-\mathbf{e}^k$ .

The exact computation of the projected probability distribution will depend on the underlying intent inference computation—for example, whether it depends on  $\mathbf{x}_r$  (which can be computed from  $\mathbf{e}^k$  applied to the robot kinematics model) or  $\mathbf{u}_h$  (which can be taken as  $\mathbf{e}^k$ ). All parameters and features which affect the computation of  $\mathbf{p}(t)$  are denoted as  $\Theta$ .

<sup>1</sup> For the rotational control dimensions, the velocity is specified with respect to the end-effector of the robotic frame.

**Algorithm 1** Calculate  $\mathbf{p}(t_b)$ ,  $\mathbf{p}(t_c)$ 


---

**Require:**  $\mathbf{p}(t_a)$ ,  $\mathbf{x}_r(t_a)$ ,  $\Delta t$ ,  $t_a < t_b < t_c$ ,  $\Theta$

```

1: for  $k = 0 \dots n_k$  do
2:   Initialize  $D_k = 0$ ,  $t = t_a$ 
3:   while  $t \leq t_c$  do
4:      $\mathbf{p}_k(t + \Delta t) \leftarrow \text{UpdateIntent}(\mathbf{p}_k(t), \mathbf{u}_h; \Theta)$ 
5:      $\mathbf{x}_r(t + \Delta t) \leftarrow \text{SimulateKinematics}(\mathbf{x}_r(t), \mathbf{u}_h)$ 
6:     if  $t = t_b$  then
7:       Compute  $\Gamma_k, \Omega_k, \Lambda_k$ 
8:     end if
9:     if  $t = t_c$  then
10:      Compute  $\Upsilon_k$ 
11:    end if
12:     $t \leftarrow t + \Delta t$ 
13:  end while
14:  Compute  $D_k$ 
15: end for

```

---

3.2.2 Components of  $D_k$ 

The computation of disambiguation metric  $D_k$  consists of four components. Each of the following components encodes some aspect of the shape of the probability distribution and is computed for projections along both positive and negative directions independently. The four components are computed in lines 7 and 10 in Algorithm 1.

1) *Maximum probability:* The maximum of the projected probability distribution  $\mathbf{p}_k(t_b)$  is a good measure of the robot’s overall certainty in accurate predicting human intent (The maximum of this discrete probability distribution is the mode of the distribution). A higher value implies that the robot has a good idea of which goal is the humans’s intended goal. We define the distribution maximum as  $\Gamma_k$ .

$$\Gamma_k = \max_{1 \leq i \leq n_g} p_k^i(t_b) \quad (1)$$

2) *Difference between largest probabilities:* Disambiguation accuracy benefits from greater differences between the first and second most probable goals. This difference is denoted as  $\Omega_k$ .

$$\Omega_k = \max(\mathbf{p}_k(t_b)) - \max(\mathbf{p}_k(t_b) \setminus \max(\mathbf{p}_k(t_b))) \quad (2)$$

3) *Pairwise separation of probabilities:* If the difference between the largest probabilities fails to disambiguate, then the separation,  $\Lambda_k$ , in the remaining goal probabilities will further aid in intent disambiguation. The quantity  $\Lambda_k$  is computed as the *sum of the pairwise distances* between the  $n_g$  probabilities.

$$\Lambda_k = \sum_{i=1}^{n_g} \sum_{j=i}^{n_g} |p_k^i(t_b) - p_k^j(t_b)| \quad (3)$$

4) *Gradients:* The probability distribution  $\mathbf{p}_k(t)$  can undergo drastic changes upon continuation of motion

along control dimension  $k$ . The spatial gradient of  $\mathbf{p}_k(t)$  encodes this propensity for change and is approximated by

$$\frac{\partial \mathbf{p}_k(t)}{\partial x_k} = \mathbf{p}_k(t_c) - \mathbf{p}_k(t_b) \quad (4)$$

where  $x_k$  is the component of robot’s displacement along control dimension  $k$ . The greater the difference between individual spatial gradients, the greater will the probabilities deviate from each other, thereby helping in disambiguation. In order to quantify the “spread” of gradients we define a quantity  $\Upsilon_k$

$$\Upsilon_k = \sum_{i=1}^{n_g} \sum_{j=i}^{n_g} \left| \frac{\partial p_k^i(t)}{\partial x_k} - \frac{\partial p_k^j(t)}{\partial x_k} \right| \quad (5)$$

where  $|\cdot|$  denotes the absolute value. *Putting it all together:*  $\Gamma_k$ ,  $\Omega_k$ ,  $\Lambda_k$  and  $\Upsilon_k$  are then combined to compute  $D_k$  as

$$D_k = \underbrace{w \cdot (\Gamma_k \cdot \Omega_k \cdot \Lambda_k)}_{\text{short-term}} + \underbrace{(1 - w) \cdot \Upsilon_k}_{\text{long-term}} \quad (6)$$

where  $w$  is a task-specific weight that balances the contributions of the short-term and long-term components. (In our implementation,  $w = 0.5$ .) Equation 6 actually is computed twice, once in each of the positive ( $e^k$ ) and negative directions ( $-e^k$ ) along  $k$ , and the results ( $D_k^+$  and  $D_k^-$ ) are then summed. The computation of  $D_k$  is performed for each control dimension  $k \in \mathcal{K}$ . The disambiguation metric  $D_m$  for control mode  $m$  then is calculated as

$$D_m = \sum_k D_k \quad (7)$$

where  $k \in m$  iterates through the set of control dimensions on which  $m$  is able to operate. Lastly, the control mode with highest disambiguation capability  $m^*$  is given by

$$m^* = \operatorname{argmax}_m D_m$$

while  $k^* = \operatorname{argmax}_k D_k$  gives the control dimension with highest disambiguation capability  $k^*$ . Disambiguation mode  $m^*$  is the mode that the algorithm chooses for the human to better estimate their intent. Any control command issued by the user in  $m^*$  is likely to be more useful for the robot in determining which is the human’s intended goal, because of the maximal confidence disambiguation.



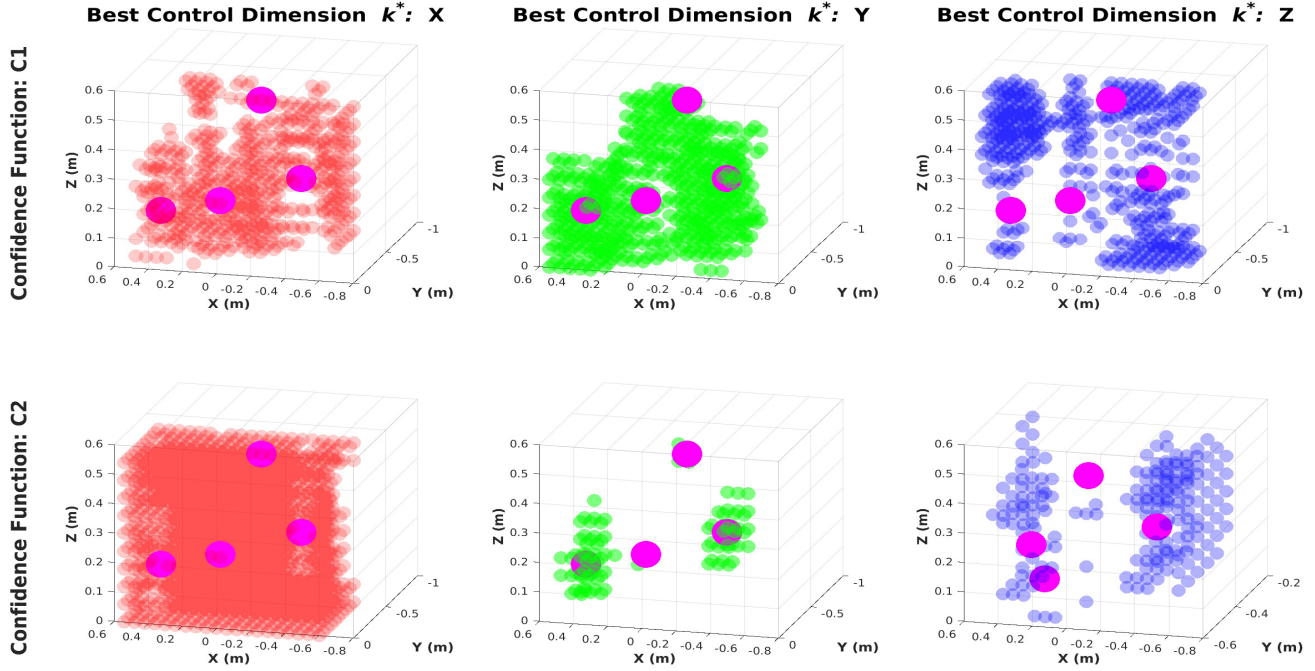


**Fig. 4** Control dimensions best able to disambiguate intent. Left column:  $k^*$  is X. Middle Column:  $k^*$  is Y. Right Column:  $k^*$  is Z. Magenta spheres indicate the goal locations (intent). In this example, the goals are spread maximally along the  $x$  and  $z$  dimensions, and so inference happens more quickly if the human control commands are along  $x$  or  $z$ . We see that  $x$  and  $z$  are chosen more often as the most disambiguating dimensions when using intent inference function C2 (bottom row). Function C2 considers the instantaneous directedness of the human’s control command towards that goal, while inference function C1 (top row) encodes only proximity to a given goal. Function C2 is considered to encode more information about the human’s intent than C1, with the result of stronger inference power—which is inherently linked to the disambiguation power of our algorithm. Further details in Gopinath and Argall (2017).

### 3.3 Intent Inference

This section describes the intent inference scheme used in this paper. Our preliminary work Gopinath and Argall (2017) revealed that the power of our disambiguation algorithm proposed in Section 3.2 is intimately linked with the inference power of different choices of intent inference mechanisms. More importantly, the pilot study associated with this preliminary work suggested that incorporating a history of past states and actions would improve performance. We therefore propose an extended disambiguation formulation which furthermore incorporates history.

In this work, we propose a novel intent inference scheme inspired by *dynamic field theory* in which the time evolution of the probability distribution  $\mathbf{p}(t)$  is specified as a dynamical system with constraints. An alternate approach is to perform intent inference using Bayesian techniques, which in theory can take into account the influence of past states and actions. In practice, however, low-order Markov assumptions are usually

made to make the inference tractable computationally, and with such assumptions history is lost.

Section 3.3.1 provides a primer on the basic principles and features of *dynamic field theory* and its application in the fields of neuroscience and cognitive robotics. Section 3.3.2 describes our novel formulation that makes use of dynamic field theory for the purposes of intent inference.

#### 3.3.1 Dynamic Field Theory

In Dynamic Field Theory (DFT) Schöner and Spencer (2015), variables of interest are treated as dynamical state variables. To represent the information about these variables requires two dimensions: one which specifies the value the variables can attain (the domain) and the other which encodes the *activation level* or the amount of information about that a particular value. These *activation fields* are analogous to probability distributions defined over a random variable.

Following Amari’s formulation Amari (1977) dynamics of an activation field  $\phi(x, t)$  are given by

$$\tau \dot{\phi}(x, t) = -\phi(x, t) + h + S(x, t) + \int dx' b(x - x') \sigma(\phi(x', t)) \quad (8)$$

where  $x$  denotes the variable of interest,  $t$  is time,  $\tau$  is the time-scale parameter,  $h$  is the constant resting level, and  $S(x, t)$  is the external input,  $b(x - x')$  is the interaction kernel and  $\sigma(\phi)$  is a sigmoidal nonlinear threshold function. The interaction kernel mediates how activations at all other field sites  $x'$  drive the activation level at  $x$ . Two types of interactions are possible: excitatory (when interaction is positive) which drives up the activation, and inhibitory (when the interaction is negative) which drives the activation down. Historically, dynamic neural fields originally were conceived to explain cortical population neuronal dynamics, based on the hypothesis that the excitatory and inhibitory neural interactions between local neuronal pools form the basis of cortical information processing Wilson and Cowan (1973).

Dynamic neural fields possess some unique characteristics that make them ideal candidates for modeling higher-level cognition. First, a peak in the activation field can be *sustained* even in the absence of external input due to the recurrent interaction terms. Second, information from the past can be *preserved* over much larger time scales quite easily by tuning the time-scale parameter thereby endowing the fields with memory. Third, the activation fields are *robust* to disturbance and noise in the external output Schöner (2008). As a result, DFT principles have found widespread application in the area of cognitive robotics Erlhagen and Bicho (2006), specifically in the contexts of efficient human-robot interaction Erlhagen and Bicho (2014), robotic scene representation Zibner et al (2011), obstacle avoidance and target reaching behaviors in both humans and robots Schöner et al (1995), and for object learning and recognition Faubel and Schöner (2008).

### 3.3.2 Dynamic Neural Fields for Intent Inference

Recurrent interaction between the state variables, robustness to noise and inherent memory make dynamic neural fields an ideal candidate for an intent inference engine. Our insight is to use the framework of dynamic neural fields to specify the time evolution of the probability distribution  $\mathbf{p}(t)$ , in which we treat the individual goal probabilities  $p^i(t)$  as constrained dynamical state variables such that  $p^i(t) \in [0, 1]$  and  $\sum_1^{n_g} p^i(t) = 1$ . The dynamical system can be generically written as

$$\dot{\mathbf{p}}(t) = F(\mathbf{p}(t), \mathbf{u}_h; \Theta) \quad (9)$$

where  $F$  represents the nonlinear vector field,  $\mathbf{u}_h$  is the human control input and  $\Theta$  represents all other task-relevant features and parameters that affect the time-evolution of the probability distribution. The full specification of the neural field is given by

$$\frac{\partial \mathbf{p}(t)}{\partial t} = \frac{1}{\tau} \left[ -\mathbb{I}_{n_g \times n_g} \cdot \mathbf{p}(t) + \underbrace{\frac{1}{n_g} \cdot \mathbb{I}_{n_g}}_{\text{rest state}} + \underbrace{\lambda_{n_g \times n_g} \cdot \sigma(\xi(\mathbf{u}_h; \Theta))}_{\text{excitatory} + \text{inhibitory}} \right] \quad (10)$$

where time-scale parameter  $\tau$  which determines the memory capacity of the system,  $\mathbb{I}$  is the identity matrix,  $\lambda$  is the control matrix that controls the excitatory and inhibitory aspects,  $\xi$  is a function that encodes the non-linearity through which human control commands and task features affect the time evolution, and  $\sigma$  is a bi-ased sigmoidal nonlinearity given by  $\sigma(\xi) = \frac{1}{1+e^{-\xi}} - 0.5$ . The off-diagonal elements of  $\lambda$  mediate the interaction between all of the probabilities. In the absence of any information or cues, the probability distribution settles to a resting state which is a uniform distribution, that is whenever  $\mathbf{u}_h = 0$ ,  $\xi = \mathbf{0}$ . Given the initial probability distribution at time  $t_a$  Equation 10 can be solved numerically from  $t \in [t_a, t_b]$  using a simple Euler algorithm with a fixed time-step  $\Delta t$ .

The design of  $\xi$  is informed by what features of the human control input and environment capture the human’s underlying intent most effectively. We rely on the *directedness* of the human control commands towards a goal, the *proximity* to a goal and the *agreement* between the human commands and robot autonomy. With  $\Theta = \{\mathbf{x}_r, \mathbf{x}_{g^i}, \mathbf{u}_{r,g^i}\}$ , one dimension  $i$  of  $\xi$  is defined as

$$\xi^i(\mathbf{u}_h; \mathbf{x}_r, \mathbf{x}_{g^i}, \mathbf{u}_{r,g^i}) = \underbrace{\frac{1+\eta}{2}}_{\text{directedness}} + \underbrace{\mathbf{u}_h^{\text{rot}} \cdot \mathbf{u}_{r,g^i}^{\text{rot}}}_{\text{agreement}} + \underbrace{\max\left(0, 1 - \frac{\|\mathbf{x}_{g^i} - \mathbf{x}_r\|}{R}\right)}_{\text{proximity}} \quad (11)$$

where  $\eta = \frac{\mathbf{u}_h^{\text{trans}} \cdot (\mathbf{x}_{g^i} - \mathbf{x}_r)^{\text{trans}}}{\|\mathbf{u}_h^{\text{trans}}\| \|(\mathbf{x}_{g^i} - \mathbf{x}_r)^{\text{trans}}\|}$ ,  $\mathbf{u}_{r,g^i}$  is the robot autonomy command for reaching goal  $g^i$ , *trans* and *rot* refer to the translational and rotational components of a command  $\mathbf{u}$  or position  $\mathbf{x}$ ,  $R$  is the radius of the sphere beyond which the proximity component is always zero, and  $\|\cdot\|$  is the Euclidean norm. That is, in the absence of any human control command, the probability distribution decays to the resting state which is a uniform distribution. The most confident goal  $g^*$  then is computed as

$$g^* = \underset{i}{\operatorname{argmax}} p^i(t) \quad (12)$$



At every time step the constraints on  $p^i(t)$  are enforced thereby ensuring that  $\mathbf{p}(t)$  is a valid probability distribution at all times.

#### 4 Shared Control

The shared control paradigm implemented on our robot is a blending-based approach in which the final control command issued to the robot is a linear composition of the human control command and an autonomous robot policy. The autonomous control policy generates control command  $\mathbf{u}_r \leftarrow f_r(\mathbf{x})$  where  $f_r(\cdot) \in \mathcal{F}_r$ , and  $\mathcal{F}_r$  is the set of all control behaviors corresponding to different tasks. This set could be derived using a variety of techniques such as *Learning from Demonstrations* Argall et al (2009); Schaal (1997), motion planners Hsu et al (2002); Ratliff et al (2009) or navigation functions Rimon and Koditschek (1992); Tanner et al (2003). Specifically, let  $\mathbf{u}_{r,g}$  be the autonomy command associated with goal  $g$ . The final control command  $\mathbf{u}$  issued to the robot then is given by

$$\mathbf{u} = \alpha \cdot \mathbf{u}_{r,g^*} + (1 - \alpha) \cdot \mathbf{u}_h$$

where  $g^*$  is the most confident goal. The blending factor  $\alpha$  is a piecewise linear function of the probability  $p(g^*)$  associated with  $g^*$  and is given by

$$\alpha = \begin{cases} 0 & p(g^*) \leq \rho_1 \\ \frac{\rho_3}{\rho_2 - \rho_1} \cdot p(g^*) & \text{if } \rho_1 < p(g^*) \leq \rho_2 \\ \rho_3 & p(g^*) > \rho_2 \end{cases}$$

with  $\rho_i \in [0, 1] \forall i \in [1, 2, 3]$  and  $\rho_2 > \rho_1$ . In our implementation, we empirically set  $\rho_1 = \frac{1.2}{n_g}$ ,  $\rho_2 = \frac{1.4}{n_g}$  and  $\rho_3 = 0.7$ . Each location  $\mathbf{x} \in \mathbb{R}^3 \times \mathbb{S}^3$  consists of a position component (3 dimensions) and orientation component (represented as a quaternion in 4 dimensions)<sup>2</sup>. Each control command  $\mathbf{u} \in \mathbb{R}^6$  consists of a translational velocity component (3 dimensions) and rotational velocity component expressed as Euler rates (3 dimensions).

The robot control command  $\mathbf{u}_{r,g}$  is generated using a simple potential field which is defined in all parts of the state space Khatib (1986). Every goal  $g$  is associated with a potential field  $\gamma_g$  which treats  $g$  as an attractor and all the other goals in the scene as repellers. For potential field  $\gamma_g$ , the attractor velocity is given by

$$\dot{\mathbf{x}}_r^{attract} = \mathbf{x}_g - \mathbf{x}_r$$

where  $\mathbf{x}_g$  is the location of goal  $g$ <sup>3</sup>. The repeller velocity is given by

$$\dot{\mathbf{x}}_r^{repel} = \sum_{i \in \mathcal{G} \setminus g} \frac{\mathbf{x}_r - \mathbf{x}_{g^i}}{\mu(\|\mathbf{x}_r - \mathbf{x}_{g^i}\|^2)}$$

where  $\dot{\mathbf{x}}_r$  indicates the velocity of the robot in the world frame,  $\mu$  controls the magnitude of the repeller velocity and  $\|\cdot\|$  is the Euclidean norm. The autonomy command is computed as a summation of these attractor and repeller velocities.

$$\mathbf{u}_{r,g} = \dot{\mathbf{x}}_r^{attract} + \dot{\mathbf{x}}_r^{repel}$$

$\gamma_g$  operates in the full six dimensional Cartesian space, and treats position and orientation as independent potential fields.

#### 5 Study Methods

In this section, we describe the study methods used to evaluate the efficacy of the disambiguation system.

##### 5.1 Participants

For this study eight subjects were recruited (mean age:  $31 \pm 11$ , 3 males and 5 females). All participants gave their informed, signed consent to participate in the experiment, which was approved by Northwestern University's Institutional Review Board.

##### 5.2 Hardware

The experiments were performed using the MICO 6-DoF robotic arm (Kinova Robotics, Canada), specifically designed for assistive purposes. The software system was implemented using the Robot Operating System (ROS) and data analysis was performed in MATLAB. The subjects teleoperated the robot using two different control interfaces: a 2-axis joystick and a switch-based head array. The control signals captured from the interfaces were mapped to the Cartesian velocities of the end-effector (Figure 5).

The joystick generated continuous control signals allowed for control of a maximum of two dimensions at a time. The 6-D control space was partitioned into four control modes that could be accessed using the buttons on the joystick interface. The switch-based head array

<sup>3</sup> In position space, the '-' operator computes the difference between the goal position and current robot position in  $\mathbb{R}^3$ . In orientation space, the '-' operator computes the *quaternion difference* between the goal orientation and the current robot orientation.

<sup>2</sup>  $\mathbb{S}^3$  is the set of all unit quaternions.

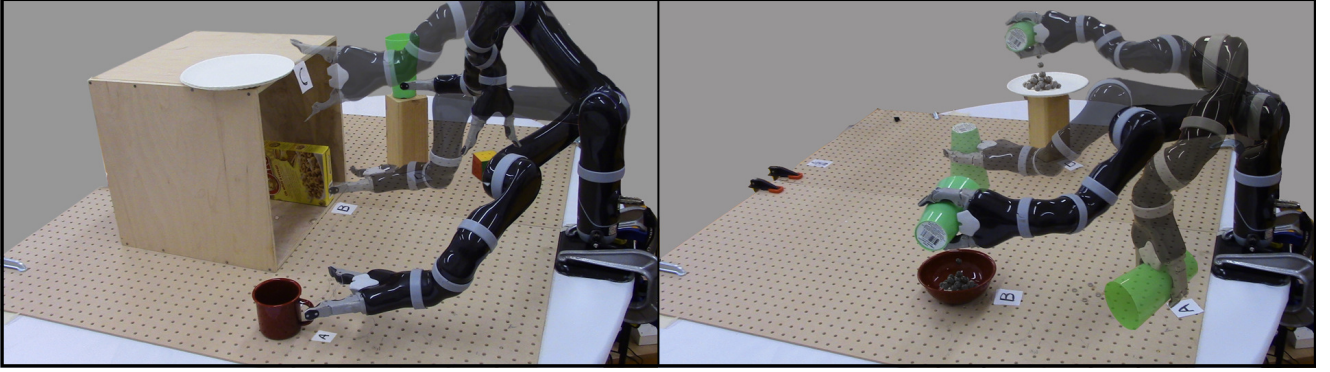



**Fig. 6** Study tasks performed by subjects. *Left*: Single-step reaching task. *Right*: Multi-step Pouring task.

consisted of three switches embedded in the headrest and generated 1-D discrete signals. The switch at the back of the headrest was used to cycle between the different control modes, and the switches to the left and right controlled the motion of the robot’s end effector in the positive and negative directions along the dimension corresponding to the selected control mode. All switches were operated via head movements. An external button was provided to request the mode switch assistance. For both control interfaces the gripper had a dedicated control mode.

### 5.2.1 Switching Paradigms

Two kinds of mode switching paradigms were evaluated in the study. Note that the blending assistance was always active for both paradigms. Under the blending paradigm, the amount of assistance was directly proportional to the probability of the most confident goal  $g^*$ , and thus to the strength of the intent inference. Therefore, if intent inference improved as a result of goal disambiguation, more assistance would be provided by the robot. All trials started in a randomized initial control mode and robot position.

**Manual:** During task execution the user performed all mode switches.



Control Mappings		
Mode	Head Array	Joystick
1	$v_x$	$v_x, v_y$
2	$v_y$	$v_x, v_z$
3	$v_z$	$\omega_z, \omega_y$
4	$\omega_z$	$\omega_x$
5	$\omega_y$	—
6	$\omega_x$	—

**Fig. 5** A 2-axis joystick (left) and switch-based head array (center) and their operational paradigms (right).  $v$  and  $\omega$  indicate the translational and rotational velocities of the end-effector, respectively.

**Disambiguation:** The user additionally could request a disambiguation mode switch at any time during task execution. Upon disambiguation request, the algorithm identified and switched the current control mode to the best disambiguating mode  $m^*$ . The user was required to request disambiguation at least once during the task execution.

### 5.3 Study Protocol

A within-subjects study was conducted using a fractional factorial design in which the manipulated variables were the tasks, control interfaces and the switching paradigm conditions. Each subject underwent an initial training period that lasted approximately thirty minutes after which the subject performed both tasks using both interfaces under the *Manual* and *Disambiguation* paradigms. The trials were balanced and the control interfaces and the paradigms were randomized and counterbalanced across all subjects to avoid ordering effects. Three trials were collected for the *Manual* paradigm and five trials for the *Disambiguation* paradigm.

**Training:** The training period consisted of three phases and two different task configurations. The subjects used both interfaces to perform the training tasks. **Phase One:** The subjects were asked to perform a simple reaching motion towards a single goal in the scene. This phase was intended for the subjects to get familiarized with the control interface mappings and teleoperation of the robotic arm.

**Phase Two:** In the second phase of training, the blending-based shared autonomy was introduced. The subjects experienced how the autonomy could provide assistance during the task execution. The subjects were informed that the robot autonomy would be present for all trials of the experiment.

**Phase Three:** For the third phase of the training, multiple objects were introduced in the scene. Subjects were informed that the robot had the capability to pick a

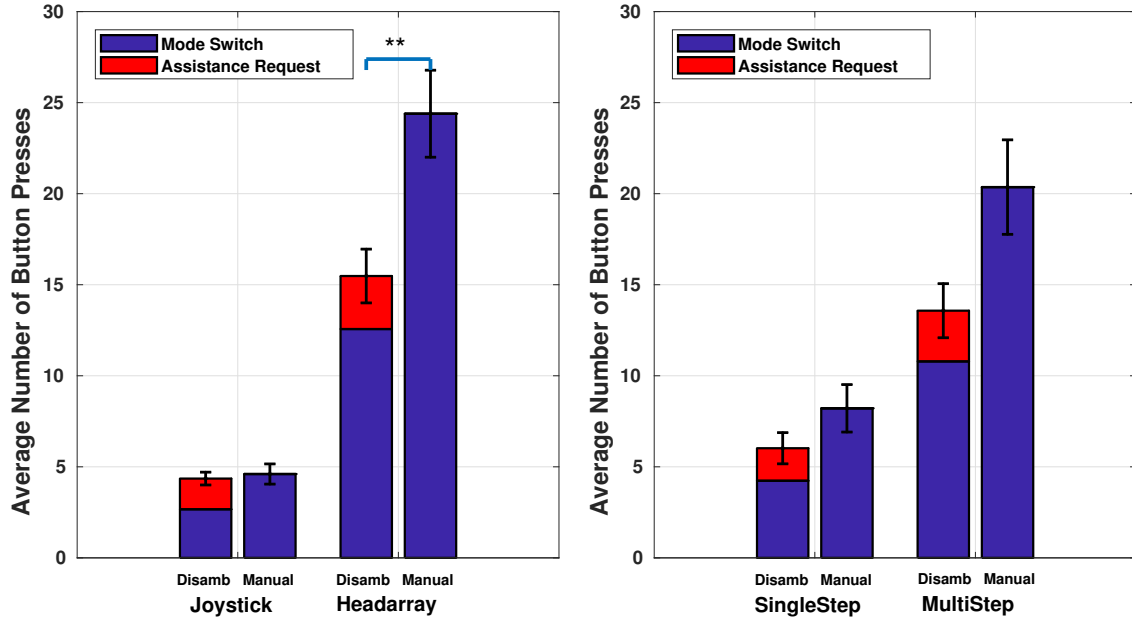


**Fig. 7** Comparison of average number of button presses between *Disambiguation* and *Manual* Paradigms. *Left*: Grouped by control interfaces. *Right*: Grouped by tasks.

control mode that would help it figure out which goal they were going for, and that the subject had the option to request the robot to pick that control mode. Subjects were able to explore this request feature during a reaching task, and were instructed to move as much as s/he can in the control mode chosen by the robot and observe the effects of the mode switch request.

**Testing:** Two different task types were evaluated during testing. Both control interfaces were employed, for all tasks.

*Single-step:* The task is to reach one of five objects on the table, each with a target orientation (Figure 6, Left).

*Multi-step:* Each trial began with a full cup held by the robot gripper. The task required first that the contents of the cup be poured into one of two containers and then that the cup be placed at one of the two specified locations and with a specific orientation (Figure 6, Right).

**Metrics:** The objective metrics used for evaluation include the following. *Number of mode switches* refers to the number of times a user switched between various control modes during task execution. *Number of assistance requests* refers to the number of times user pressed the button requesting disambiguating assistance. *Number of button presses* is the sum of *Number of mode switches* and *Number of assistance requests*, and is also an indirect measure of user effort. We also characterize the temporal distribution of assistance requests.

## 6 Results

Here we report the results of our subject study. Statistical significance is determined by the Wilcoxon Rank-Sum test in Figure 7 where (\*\*\*) indicates  $p < 0.001$ , (\*\*)  $p < 0.01$  and (\*)  $p < 0.05$ .

### 6.1 Impact of Disambiguation on Task Performance

A statistically significant improvement in task performance in terms of a decrease in the number of button presses was observed between the *Manual* and *Disambiguation* paradigms when using the headarray (Figure 7, Left). Due to the low-dimensionality of headarray and cyclical nature of mode switching, the number of button presses required for task completion is inherently high. The disambiguation paradigm was helpful in reducing the number of button presses likely due to the fact that robot assistance was more effective in the disambiguating control mode and therefore reduced the need for subsequent user-initiated mode switches which in turn would have helped in reducing the task effort. For joystick, although statistically significant differences were observed for the number of mode switches between the two paradigms the gain due to the reduction of user-initiated mode switches was offset by the button presses that were required for assistance requests. A general trend (although not statistically significant) of a decrease in the number of button presses was also

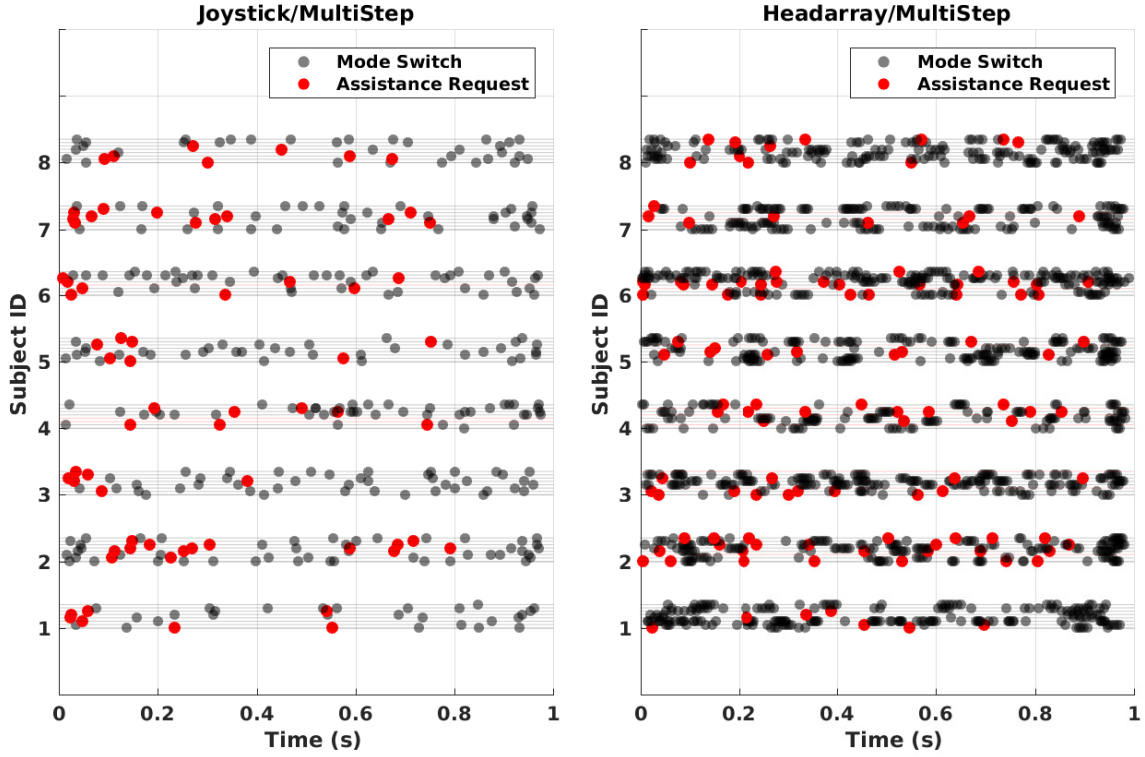


**Fig. 8** Temporal pattern of button presses for each interface/task combination on a trial-by-trial basis for all subjects. Eight trials per subject per interface/task combination. Gray and red horizontal lines denote successful and unsuccessful trials respectively.

observed for the more complex multi-step task (Figure 7, Right). That is, subjects found most utility for the disambiguation paradigm when the control interface was more limited and the task was more complex.

## 6.2 Temporal Distribution of Disambiguation Requests

We also observed similar correlations between the *temporal distribution* of disambiguation requests and the type of interface/task combinations. The temporal distribution of disambiguation requests refers to *when* the subject requested assistance during the course of a trial. We use a measure of *skewness* to characterize how much the temporal distribution deviates from a uniform distribution.<sup>4</sup> A positive value of skewness indicates that assistance requests are more concentrated to the earlier parts of the trials. Higher the skewness the more concentrated they are. Table 1 reports the skewness of the temporal distribution of assistance requests for different interface/task combinations. We observed that

<sup>4</sup> A uniform temporal distribution corresponds to a trial in which the assistance requests are uniformly spread out during the course of task execution. The skewness of a uniform distribution is 0.

the assistance requests became more uniform (decreasing skewness values) as the interface/task combination became harder. The need for assistance is more persistent for these combinations and as a result the subjects would have utilized the disambiguation paradigm more evenly throughout the course of the trial.

Figure 8 shows the temporal pattern for disambiguation requests and mode switches for the multi-step for both interfaces on a trial-by-trial basis for all subjects. From the figure it is clear that the frequency and density of button presses (both assistance requests and mode switches) are much higher for the more limited control interface. The subjects also demonstrated a diverse range of button press behavior. Some subjects preferred to perform manual mode switches to requesting assistance (e.g. Subject 1) whereas some others utilized the assistance paradigm a great deal more (e.g Subject 2). The variation between subjects is likely due to different factors such as the user’s comfort in operating the robot and understanding the effectiveness of robot assistance in the disambiguating mode.

	Single Step	Multi Step
Joystick	0.63	0.57
Headarray	0.35	0.22

**Table 1** Characterization of the temporal distribution of assistance requests. The values in the table denotes the deviation of the temporal distribution from a uniform distribution. This deviation is captured using the *Skewness* measure.

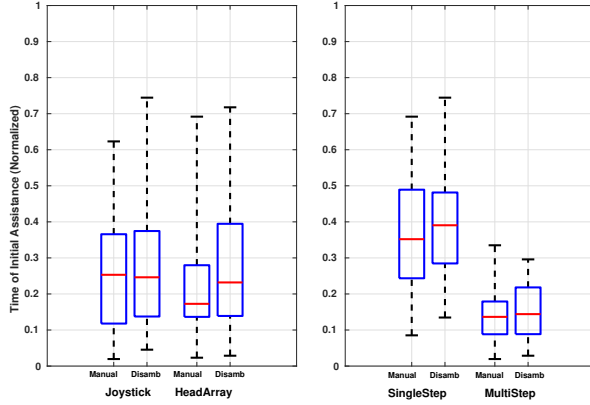


**Fig. 9** Onset of robot assistance normalized with respect to task completion time. *Left*: Across interfaces. *Right*: Across tasks.

### 6.3 Onset of Robot Assistance

Our motivating intuition for developing the disambiguation system was that for disambiguation trials the robot assistance will step in earlier during the course of task execution. However, our results did not reveal any statistically significant differences between the two assistance paradigms across tasks and across interfaces (Figure 9). We think there are two plausible explanations for this. Firstly, subjects chose not to operate in the disambiguating modes and therefore did not ‘help’ the robot in intent inference due to which the robot’s confidence never passed the minimum threshold for assistance to step in.

Secondly, it was also possible that the training period was not sufficient enough for the subjects to gain a good grasp on what aspects of task execution did the robot rely on to provide assistance. Therefore, the subjects might not have had any incentive to operate in the disambiguating mode.

Figure 10 illustrates two very different approaches to performing the task and their impact on robot assistance. Subject A (Figure 10 (Top)) operated the robot in a more continuous fashion and chose to operate the robot in the disambiguating mode and thereby resulted in a sharp rise in goal confidence. On the other hand, Subject B operated the robot more sparsely and as a result the goal confidence did not cross the minimum threshold required for assistance. Despite the greater number of assistance requests, Subject B was not able to leverage

the benefits of operating in a disambiguating mode and therefore the robot assistance was not able to step in earlier to help the user.

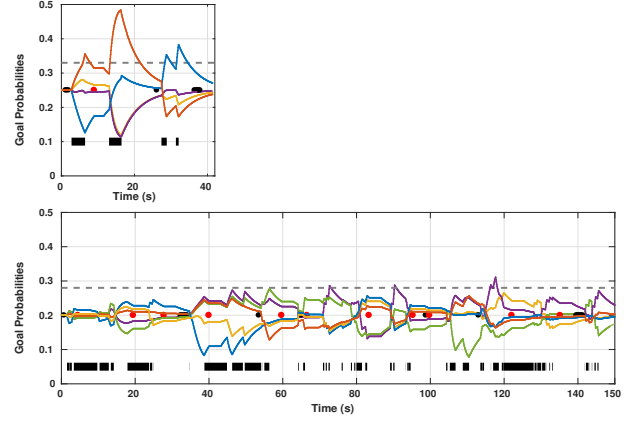


**Fig. 10** Time evolution of goal probabilities. *Top*: Multi-step task. *Bottom*: Single-step task. The gray horizontal line above denotes the minimum threshold for robot assistance. The thick black line at the bottom denotes non-zero human control commands. The red and black dots indicate button presses that are assistance requests and mode switches respectively.

## 7 Discussion

In a *help me, help you* type of human robot system, task execution becomes seamless and more efficient when there is a sound mutual understanding of how the other party operates. The robot uses its own intent inference engine to understand the human’s intent. However, when subjects vary in responding to the training sessions, they also vary in their understanding of the robot’s assistance. The knowledge of robot’s assistance mechanism is paramount for the user to provide *intent-expressive* control commands for the robot.

Therefore, the need for extensive and thorough training becomes apparent. The training can be made more effective in a few different ways—First, online feedback of the robot’s intent prediction at all times during training can likely help the subject gain a better understanding of the relationship between the characteristics of their control actions (sparsity, aggressiveness, persistence) and the robot’s assistive behavior. Second, the subjects could be explicitly informed of the task relevant features (directedness, proximity *et cetera*) that the robot relies on for determining the amount of assistance. Knowledge of these features might motivate the users to leverage the advantages of operating the robot in the disambiguating mode.



The inherent time delays associated with the computation of the disambiguating mode (approximately 2-2.5s) might have been a discouraging factor and a cause for user frustration. The algorithm could be used to pre-compute a large set of most informative modes for different parts of the workspace, for different goal configurations and for different priors ahead of time, which then might be used a lookup table during task execution. Furthermore, metamodeling techniques and machine learning tools can be used to learn generalizable models that will be effective in previously unseen goal configurations.

In the present system, there is task effort associated with requesting assistance which can discourage the users from utilizing assistance. Automated mode switching schemes can possibly eliminate the need for button presses for assistance requests. We also identify an opportunity to have adaptive assistance paradigms that explicitly take into account the characteristics of the user's control behavior. Some users are timid in their operation of the robot whereas some others are more aggressive and confident. Some are more comfortable operating the robot manually and do not seek assistance, whereas some others rely on assistance more frequently. Individual user characteristics could be extracted from the training data and be used for tuning the parameters of the intent inference engine and the shared control system to maximize robustness and efficacy of the assistive system. This would also likely improve user satisfaction and result in higher user acceptance.

## 8 Conclusion

In this paper, we have presented an algorithm for *intent disambiguation assistance* with a shared-control robotic arm using the notion of *inverse legibility*. The goal of this algorithm is to elicit more *intent-expressive* control commands from the user by placing control in those control modes that *maximally disambiguate* between the various goals in the scene. As a secondary contribution, we also present a novel intent inference mechanism inspired by *dynamic field theory* that works in conjunction with the disambiguation system. A user study was conducted with eight subjects to evaluate the efficacy of the disambiguation system. Our results indicate a decrease in task effort in terms of the number of button presses when disambiguation system employed.

## References

- Amari Si (1977) Dynamics of pattern formation in lateral-inhibition type neural fields. *Biological Cybernetics* 27(2):77–87
- Argall BD, Chernova S, Veloso M, Browning B (2009) A survey of robot learning from demonstration. *Robotics and Autonomous Systems* 57(5):469–483
- Atanasov N, Le Ny J, Daniilidis K, Pappas GJ (2014) Information acquisition with sensing robots: Algorithms and error bounds. In: *Proceedings of the IEEE International Conference on Robotics and Automation (ICRA)*
- Calinon S, Li Z, Alizadeh T, Tsagarakis NG, Caldwell DG (2012) Statistical dynamical systems for skills acquisition in humanoids. In: *Proceedings of the 12th IEEE-RAS International Conference on Humanoid Robots (Humanoids)*, IEEE, pp 323–329
- Choi YS, Anderson CD, Glass JD, Kemp CC (2008) Laser pointers and a touch screen: intuitive interfaces for autonomous mobile manipulation for the motor impaired. In: *Proceedings of the International SIGACCESS Conference on Computers and Accessibility*
- Demeester E, Hüntemann A, Vanhooydonck D, Vanacker G, Van Brussel H, Nuttin M (2008) User-adapted plan recognition and user-adapted shared control: A bayesian approach to semi-autonomous wheelchair driving. *Autonomous Robots* 24(2):193–211
- Downey JE, Weiss JM, Mueller K, Venkatraman A, Valois JS, Hebert M, Bagnell JA, Schwartz AB, Collinger JL (2016) Blending of brain-machine interface and vision-guided autonomous robotics improves neuro-prosthetic arm performance during grasping. *Journal of Neuroengineering and Rehabilitation* 13(1):28
- Dragan AD, Srinivasa SS (2012) Assistive teleoperation for manipulation tasks. In: *Proceedings of ACM/IEEE International Conference on Human-Robot Interaction (HRI)*
- Dragan AD, Lee KC, Srinivasa SS (2013) Legibility and predictability of robot motion. In: *Proceedings of the ACM/IEEE International Conference on Human-Robot Interaction (HRI)*
- Driessen B, Kate TT, Liefhebber F, Versluis A, Van Wierden J (2005) Collaborative control of the manus manipulator. *Universal Access in the Information Society* 4(2):165–173
- Eftiring H, Boschian K (1999) Technical results from manus user trials. In: *IEEE 2nd International Conference on Rehabilitation Robotics (ICORR)*
- Erlhagen W, Bicho E (2006) The dynamic neural field approach to cognitive robotics. *Journal of Neural Engineering* 3(3):R36
- Erlhagen W, Bicho E (2014) A dynamic neural field approach to natural and efficient human-robot collaboration. In: *Neural Fields*, Springer, pp 341–365
- Faubel C, Schöner G (2008) Learning to recognize objects on the fly: a neurally based dynamic field approach. *Neural Networks* 21(4):562–576



- Goodfellow IJ, Koenig N, Muja M, Pantofaru C, Sorokin A, Takayama L (2010) Help me help you: Interfaces for personal robots. In: *Proceedings of ACM/IEEE International Conference on Human-Robot Interaction (HRI)*
- Gopinath D, Argall B (2017) Mode switch assistance to maximize human intent disambiguation. In: *Robotics: Science and Systems*
- Gopinath D, Jain S, Argall BD (2017) Human-in-the-loop optimization of shared autonomy in assistive robotics. *IEEE Robotics and Automation Letters* 2(1):247–254
- Herlant LV, Holladay RM, Srinivasa SS (2016) Assistive teleoperation of robot arms via automatic time-optimal mode switching. In: *Proceedings of the ACM/IEEE International Conference on Human-Robot Interaction (HRI)*
- Holladay RM, Dragan AD, Srinivasa SS (2014) Legible robot pointing. In: *The IEEE International Symposium on Robot and Human Interactive Communication (RO-MAN)*
- Hsu D, Kindel R, Latombe JC, Rock S (2002) Randomized kinodynamic motion planning with moving obstacles. *The International Journal of Robotics Research* 21(3):233–255
- Huete AJ, Victores JG, Martinez S, Giménez A, Balaguer C (2012) Personal autonomy rehabilitation in home environments by a portable assistive robot. *IEEE Transactions on Systems, Man, and Cybernetics, Part C (Applications and Reviews)* 42(4):561–570
- Khansari-Zadeh SM, Billard A (2011) Learning stable nonlinear dynamical systems with gaussian mixture models. *IEEE Transactions on Robotics* 27(5):943–957
- Khatib O (1986) Real-time obstacle avoidance for manipulators and mobile robots. *The International Journal of Robotics Research* 5(1):90–98
- Kim DJ, Hazlett R, Godfrey H, Rucks G, Portee D, Bricout J, Cunningham T, Behal A (2010) On the relationship between autonomy, performance, and satisfaction: Lessons from a three-week user study with post-sci patients using a smart 6dof assistive robotic manipulator. In: *Proceeding of the IEEE International Conference on Robotics and Automation (ICRA)*, IEEE, pp 217–222
- Kim DJ, Hazlett-Knudsen R, Culver-Godfrey H, Rucks G, Cunningham T, Portee D, Bricout J, Wang Z, Behal A (2012) How autonomy impacts performance and satisfaction: Results from a study with spinal cord injured subjects using an assistive robot. *IEEE Transactions on Systems, Man, and Cybernetics-Part A: Systems and Humans* 42(1):2–14
- LaPlante MP, et al (1992) Assistive technology devices and home accessibility features: prevalence, payment, need, and trends. *Advance Data from Vital and Health Statistics*
- Liu C, Hamrick JB, Fisac JF, Dragan AD, Hedrick JK, Sastry SS, Griffiths TL (2016) Goal inference improves objective and perceived performance in human-robot collaboration. In: *Proceedings of the 2016 International Conference on Autonomous Agents & Multiagent Systems*, International Foundation for Autonomous Agents and Multiagent Systems, pp 940–948
- Miller LM, Murphey TD (2013) Trajectory optimization for continuous ergodic exploration. In: *American Control Conference (ACC)*
- Miller LM, Silverman Y, MacIver MA, Murphey TD (2016) Ergodic exploration of distributed information. *IEEE Transactions on Robotics* 32(1):36–52
- Muelling K, Venkatraman A, Valois JS, Downey JE, Weiss J, Javdani S, Hebert M, Schwartz AB, Collinger JL, Bagnell JA (2017) Autonomy infused teleoperation with application to brain computer interface controlled manipulation. *Autonomous Robots* pp 1–22
- Nuttin M, Vanhooydonck D, Demeester E, Van Brussel H (2002) Selection of suitable human-robot interaction techniques for intelligent wheelchairs. In: *Proceedings of 11th IEEE International Workshop on Robot and Human Interactive Communication*, IEEE, pp 146–151
- Philips J, Millán JdR, Vanacker G, Lew E, Galán F, Ferrez PW, Van Brussel H, Nuttin M (2007) Adaptive shared control of a brain-actuated simulated wheelchair. In: *Proceedings of the IEEE International Conference on Rehabilitation Robotics (ICORR)*, IEEE, pp 408–414
- Pilarski PM, Dawson MR, Degris T, Carey JP, Sutton RS (2012) Dynamic switching and real-time machine learning for improved human control of assistive biomedical robots. In: *Proceedings of the IEEE RAS & EMBS International Conference on Biomedical Robotics and Biomechatronics (BioRob)*, IEEE, pp 296–302
- Ratliff N, Zucker M, Bagnell JA, Srinivasa S (2009) Chomp: Gradient optimization techniques for efficient motion planning. In: *Proceedings of the IEEE International Conference on Robotics and Automation (ICRA)*, IEEE, pp 489–494
- Rimon E, Koditschek DE (1992) Exact robot navigation using artificial potential functions. *IEEE Transactions on Robotics and Automation* 8(5):501–518
- Sadigh D, Sastry S, Seshia SA, Dragan AD (2016a) Planning for autonomous cars that leverage effects on human actions. In: *Robotics: Science and Systems*

- Sadigh D, Sastry SS, Seshia SA, Dragan A (2016b) Information gathering actions over human internal state. In: *Proceedings of the IEEE/RSJ International Conference on Intelligent Robots and Systems (IROS)*, IEEE, pp 66–73
- Schaal S (1997) Learning from demonstration. In: *Advances in Neural Information Processing Systems*, pp 1040–1046
- Scherer MJ (1996) Outcomes of assistive technology use on quality of life. *Disability and Rehabilitation* 18(9):439–448
- Schöner G (2008) Dynamical systems approaches to cognition. *Cambridge Handbook of Computational Cognitive Modeling* pp 101–126
- Schöner G, Spencer J (2015) *Dynamic thinking: A primer on dynamic field theory*. Oxford University Press
- Schöner G, Dose M, Engels C (1995) Dynamics of behavior: Theory and applications for autonomous robot architectures. *Robotics and Autonomous Systems* 16(2-4):213–245
- Simpson T, Broughton C, Gauthier MJ, Prochazka A (2008) Tooth-click control of a hands-free computer interface. *IEEE Transactions on Biomedical Engineering* 55(8):2050–2056
- Sorokin A, Berenson D, Srinivasa SS, Hebert M (2010) People helping robots helping people: Crowdsourcing for grasping novel objects. In: *Proceedings of the IEEE/RSJ International Conference on Intelligent Robots and Systems (IROS)*
- Storms JG, Tilbury DM (2014) Blending of human and obstacle avoidance control for a high speed mobile robot. In: *American Control Conference (ACC)*, IEEE, pp 3488–3493
- Taha T, Miró JV, Dissanayake G (2011) A pomdp framework for modelling human interaction with assistive robots. In: *Proceedings of the IEEE International Conference on Robotics and Automation (ICRA)*, IEEE, pp 544–549
- Tanner HG, Loizou SG, Kyriakopoulos KJ (2003) Non-holonomic navigation and control of cooperating mobile manipulators. *IEEE Transactions on Robotics and Automation* 19(1):53–64
- Tomasello M, Carpenter M (2007) Shared intentionality. *Developmental Science* 10(1):121–125
- Tomasello M, Moll H (2010) The gap is social: Human shared intentionality and culture. In: *Mind the Gap*, Springer, pp 331–349
- Tsui KM, Kim DJ, Behal A, Kontak D, Yanco HA (2011) I want that: Human-in-the-loop control of a wheelchair-mounted robotic arm. *Applied Bionics and Biomechanics* 8(1):127–147
- Wilson HR, Cowan JD (1973) A mathematical theory of the functional dynamics of cortical and thalamic nervous tissue. *Biological Cybernetics* 13(2):55–80
- Zibner SK, Faubel C, Iossifidis I, Schöner G (2011) Dynamic neural fields as building blocks of a cortex-inspired architecture for robotic scene representation. *IEEE Transactions on Autonomous Mental Development* 3(1):74–91